

Long-chain *syn*-1-phenylalkane-1,3-diyl diacetates, related phenylalkane derivatives, and *sec*-alcohols, all possessing dominantly *iso*-branched chain termini, and 2/3-methyl-branched fatty acids from *Primula veris* L. (Primulaceae) wax

Niko S. Radulović^{*}, Milena Z. Živković Stošić

Department of Chemistry, Faculty of Sciences and Mathematics, University of Niš, Višegradska 33, 18000, Niš, Serbia

ARTICLE INFO

Keywords:

Primula veris L.
Primulaceae
Branched long-chain wax constituents
syn-1-Phenylalkane-1,3-diyl diacetates
3-Oxo-1-phenylalkan-1-yl acetates
1-Phenylalkane-1,3-diones
sec-Alcohols
2-Methylalkanoic and 3-methylalkanoic acids

ABSTRACT

Herein, the results of the first study of non-flavonoid constituents of aboveground surface-wax washings of *Primula veris* L. (Primulaceae) are presented. Chromatography of the washings yielded a minor fraction composed of *n*-, *iso*-, and *anteiso*-series of long-chained *syn*-1-phenylalkane-1,3-diyl diacetates, 3-oxo-1-phenylalkan-1-yl acetates, 1-phenylalkane-1,3-diones, 1-hydroxy-1-phenylalkan-3-ones, *sec*-alcohols (2- to 10-alkanols), and *n*-, *iso*-, *anteiso*-, 2-methylalkanoic and 3-methylalkanoic acids; 118 of these constituents represent up to now unreported natural compounds. The structural/stereochemical elucidation was accomplished by the synthesis of authentic standards, derivatization reactions, the use of gas chromatographic retention data and detailed 1D and 2D-NMR analyses of the obtained complex chromatographic fraction. *Primula veris* produces unusually high amounts of branched long-chained metabolites (>60%) except for the fatty acids where the percentage of branched isomers is comparable to the ones with *n*-chains. Noteworthy is the fact that long-chained α - and β -methyl substituted fatty acids were detected herein for the first time in the kingdom Plantae.

1. Introduction

Aerial organs of land plants are covered by a cuticle that primarily protects the organ from non-stomatal water loss. This waxy composite represents a complex mixture of predominantly very-long-chain (VLC) compounds whose structure defines the functional properties of the barrier with respect to the surrounding environment (Jetter et al., 2006). The epicuticular waxes form the outmost layers that are most frequently composed of non-polar VLC homologous series of compounds containing no functional groups (alkanes) or a single functional group at or near the chain termini (1- or 2-alkanols, aldehydes, 2-alkanones, esters, etc.). Overwhelmingly, these chains were reported to be unbranched, but if branches are present, these are usually compounds of low abundance (compared to the linear counterparts) with methyl groups located at the very end of the chains (*iso*-series) or next to it (*anteiso*-series). Thus, the branched-chain compounds are not only found in low amounts but are also exceedingly rare in the classes of wax constituents other than alkanes. Up to now only branched primary alcohols, fatty acids and their esters have been detected (Jetter et al., 2006; Busta and Jetter, 2017;

Dekić et al., 2019).

The most valuable analytical technique employed for the identification and quantification of single wax VLC constituents is gas chromatography (GC) alone or coupled with mass spectrometry (GC-MS). The reasons behind the underutilization of other (liquid) chromatographic and spectral (e.g., NMR, IR, and UV) methods are the difficult or impossible separations on standard stationary phases due to the very similar polarity within the mixture of constituents belonging to a specific class, and non-informativeness of the spectra of these mixtures (data on single compounds are lost due to signal overlap, while the positioning of functional groups that are far from the chain termini cannot be inferred due to almost complete signal isochronicity). Additionally, in general, GC and GC-MS analyses are complicated by the lack of VLC commercial reference compounds and especially of most branched VLC compounds (the exceptions are branched fatty acids, mostly *iso*- and *anteiso*-chained, which are commercially accessible). This means that the researchers in this field usually need to turn to organic synthesis to obtain such standards or must devise other more elaborate means (a combination of approaches including derivatization

^{*} Corresponding author.

E-mail address: nikoradulovic@yahoo.com (N.S. Radulović).

reactions; Busta and Jetter, 2017; Dekić et al., 2019).

Structural elucidation of secondary metabolites usually requires an access to a sample of sufficient purity to permit NMR analyses. In the case of long-chain compounds, encountered in wax constituents, both requirements are very difficult or impossible to meet. Homologous compounds differ only minutely in their polarity and cannot be separated using conventional liquid chromatography but are easily discerned by gas chromatography. The long chains result in shift isochronicity and obstruct locating appropriate correlations in 2D NMR spectra that would produce connectivity data needed. For example, a functional group at one chain terminus cannot be brought into direct link via NMR with the other terminus. However, when one measures an NMR spectrum of a mixture of homologous compounds the difference in the chemical shifts among the long-chained homologous is usually negligible. Logically, the mass spectra are crucial in piecing the molecule together, but these cannot be easily used to differentiate among isomers. Thus, a third characteristic is necessary, which would allow specific combinations of isomeric moieties to be interconnected. Gas chromatography offers this unique tool, the retention indices, which can distinguish close positional isomers based on their different volatility. However, these are not easily attainable or are non-existent in the literature in the case of rare or new metabolites, and this problem can be only solved by employing synthesis of the very metabolites or their homologs.

The genus *Primula* L. is the largest genus among the Primulaceae and includes more than 400 species distributed throughout the cold and temperate regions of the Northern Hemisphere (Colombo et al., 2017). The production of oily or farinose exudates (farina) on aerial surfaces of leaves, stems, calyces, and inflorescences is universal among *Primula* taxa with glandular trichomes. *Primula* L. is one of the most widespread of all plant genera, possibly because of its successful adaptation to extreme environmental conditions (high altitudes, low temperatures, high level of ionizing radiation, aridity, etc.; Richards, 2003; Zhang et al., 2013). These exudates consist primarily of unsubstituted flavone accompanied by a series of other highly unusual, methoxylated flavones lacking the typical oxygenations, some of which are substituted by a single hydroxyl or methoxyl group (Bhutia and Valant-Vetschera, 2012; Berim and Gang, 2015).

Although several phytochemical studies devoted to the analyses of the chemical composition of *Primula* glandular trichome exudates have been carried out in the last decades (Huck et al., 2000; Bhutia et al., 2013; Berim and Gang, 2015; Shostak et al., 2016; Colombo et al., 2017), these offer limited data on the non-flavonoid constituents. So far, only one diterpene (*ent*-kaur-16-en-19-oic acid; Elser et al., 2016), two dihydrochalcones (Bhutia et al., 2013), and three chalcones (Wollenweber et al., 1989; Budzianowski and Wollenweber, 2007; Valant-Vetschera et al., 2009) have been reported thereof. One of the most renowned plant species from this genus is *Primula veris* L. that was the subject of phytochemical and pharmacological (Aslam et al., 2014; Chinou et al., 2014) studies on numerous occasions and found its place in several pharmacopoeias: *Primulae flos* and *Primulae radix* (British Herbal Medicine Association, 1974; L'Adapharm, 1988; Council of Europe, 2019). Most recently, for the first time discovered in a natural source, several flavones, substituted only in the B ring, have been found in the wax of *P. veris* (Budzianowski et al., 2005). The waxes/farinas of this taxon have been investigated for the presence/structural elucidation of flavonoids from several regions (Valant-Vetschera et al., 2009; Shostak et al., 2016; Apel et al., 2017; Bączek et al., 2017), but never previously from Serbia.

In this work, the focus was directed at non-flavonoid-type constituents of waxy exudates from the entire plants in bloom since these have been neglected entirely. The interest in these minor wax constituents came from one of our preliminary studies on alkanes of *P. veris* and *P. acaulis* L. (L.), which were characterized by a very high contribution of branched alkanes compared to the linear isomers (Živković et al., 2016). For this reason, chloroform washings of the entire intact blooming plants were chromatographically separated and analyzed by GC-MS, with or

without prior derivatization, and subsequently extensively by NMR. Along with the expected flavonoid derivatives, which were not the subject of this work, a very minor fraction, ca. 12 mg of which were at hand, proved to be a prolific source of new constituents that possessed unusual chain functionalization, the number and identity of functional groups, in addition to having *iso*- and *anteiso*-branches at chain termini, or branches in α - or β -position to the functional group. The identification of these plant metabolites would not have been possible without the synthetic endeavors to produce analogs used for both direct comparisons of spectral data and predicting of retention indices of higher homologs. In the current study, in total 16 unreported *syn*-1-phenyl-1,3-alkanediyl diacetates, 7 unreported 3-oxo-1-phenylalkan-1-yl acetates, 8 unreported 1-phenylalkane-1,3-diones, 10 unreported 1-hydroxy-1-phenylalkan-3-ones, 66 unreported *sec*-alkanols, 11 unreported (ω -1)-, (ω -2)-, 2- or 3-methylalkanoic acids were identified. Except for the acids, all other identified classes were present as both *n*-, *iso*- and *anteiso*-isomers at chain ends with the *iso*-isomer being the predominant one. This work gives an account of the structural elucidation of these compounds that was specific due to the VLC-nature of the constituents, the low available amount of the material and impossibility of further separation.

2. Results and discussion

2.1. 1-Phenylalkane-1,3-diyl diacetates

The most dominant peaks in the GC-MS chromatogram of the fraction displayed mass spectra having prominent ions at m/z 43 [CH_3CO]⁺, as the base peak, and at m/z 105 [PhCO]⁺, suggesting the presence of one or more acetyl groups in their structure, and of a monosubstituted phenyl group possessing an oxygenation in the benzylic position. Sixteen compounds showed this MS pattern, and these were distributed into three series having an approximate increment of ca. 101 RI units per CH_2 group, (SI, Table S3; Figure S1), implying three different chain termini. Our NMR entrance points, bearing in mind that these are NMRs of the entire fraction, for this group of compounds were the recognizable singlets of methyl groups within acetates, at 2.06 and 1.98 ppm (Fig. 1), attached to carbon atoms at 21.2 and 21.3 ppm (SI, Figure S3), which also correlated with ester carbonyls at 170.5 and 170.1 ppm via two bonds (gHMBC). The only other long-range C–H correlations of these carbonyls were to a pseudo triplet at 5.79 ppm (dd, $J = 7.15, 6.70$ Hz, H_a) and a complex multiplet at 4.78 ppm (dddd, $J = 8.36, 6.30, 6.20, 4.50$ Hz, H_d), respectively (Table 1). The two esterified carbinol C–H were separated by only a single CH_2 group (2.03 ppm, ddd, $J = -14.52, 6.70, 4.50$ Hz, H_b and 2.23 ppm, ddd, $J = -14.52, 8.36, 7.15$ Hz, H_c) judged from the observed ^1H – ^1H COSY, NOESY, and gHMBC interactions (Fig. 1B and C). gHMBC and NOESY provided further links of the H_a proton to a phenyl group geminal to one of the acetates, while the H_d proton was adjacent to an alkyl chain. Thus, the molecules contained at one terminus the 1-phenylalkane-1,3-diyl diacetate moiety while the other terminus should be the branched or non-branched alkyl chains (SI, Figure S2; Table S2). The observed fragmentation patterns in the MS of the wax constituents could now be readily interpreted, as presented in the SI material (SI, Table S4; Figures S4-1 – S4-8).

Since there are at least two chiral centers in the molecule (two for *n*- and *iso*-branched chains, and three from the *anteiso*-branched chains), two (i.e. four) diastereoisomers are possible, which are frequently, but not unambiguously, designated as *syn* ($1S^*,3S^*$) and *anti* ($1S^*,3R^*$) (Fig. 3, Moss, 1996). To resolve the splitting patterns of H_a , H_b , H_c , and H_d , the spin system was simulated (Radulović et al., 2019) using Mestrelab Research S.L. (MestReNova) software package (Fig. 1), with the aim of inferring the relative configuration from the values of the pertinent coupling constants; this would also allow to additionally separate the signals of these diacetates from the overlapping signals coming from the other constituents of the fraction. The chemical shifts and the extracted values of the coupling constants were compared with the data

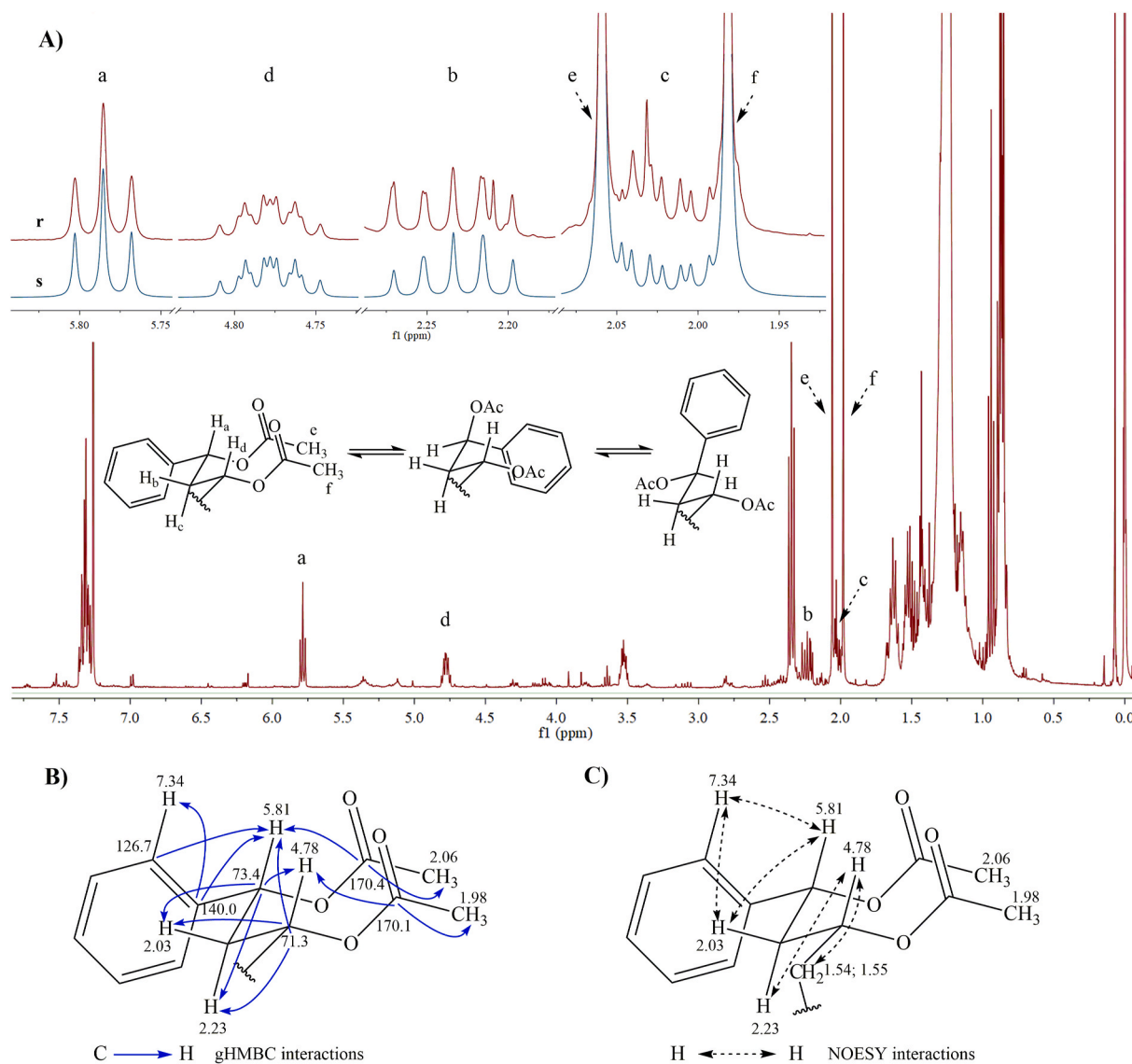


Fig. 1. A) ^1H NMR spectrum of a chromatographic fraction of *P. veris* aboveground wax with expansions of signals (maroon trace) belonging to *syn*-1-phenylalkane-1,3-diyl diacetates (*syn*-1a, 2a-c, 3a-b, 4a-c, 5a-b, 6a-c, and 7a-b, signals a-f). “s” trace (blue) gives the simulated signals of these wax constituents, while “r” represents the corresponding experimental spectrum expansions; B) and C) observed crucial gHMBC and NOESY interactions of *syn*-1-phenylalkane-1,3-diyl diacetates (*syn*-1a, 2a-c, 3a-b, 4a-c, 5a-b, 6a-c, and 7a-b). (For interpretation of the references to colour in this figure legend, the reader is referred to the Web version of this article.)

available in the literature for the related systems. Although, considerable knowledge (Hoffmann and Weidmann, 1985; Pelter et al., 1993) is accumulated in the case of *syn*- and *anti*-diols, which can permit differentiation of these diastereoisomers, such spectral tools could only be used when ^{13}C NMR data are accessible for both isomers. Likewise, specific data on *syn*- and *anti*-1-aryl-1,3-alkanediyl diesters are exceedingly rare and the only comparable and useful ones are given in Table 1 and Fig. 3 ((1*S*,3*S*)-1,5-diphenylpentane-1,3-diyl diacetate (*syn* isomer) and (1*S*,3*R*)-1,5-diphenylpentane-1,3-diyl dipropionate (*anti* isomer); compounds 10 and 11, Niwa et al., 1987; Merad et al., 2017). The comparison of our data for both ^1H NMR chemical shifts and coupling constant values with the literature data of the two synthetic compounds strongly pointed to the *syn*-relative configuration of the diacetates from *P. veris*.

This tentative relative stereochemical assignment was confirmed in two ways. At first, a short model compound, 1-phenyl-1,3-butanediyl diacetate (8a, SI, chapter 2.2.), was synthesized starting from the commercially available 1-phenylbutane-1,3-dione (28a) through the

reduction with NaBH_4 to the corresponding diols, and subsequent esterification. The relative configuration of the intermediary *syn*- and *anti*-diols (12a, Figure S5, SI) was established from further experiments involving the formation of cyclic acetals with benzaldehyde. These benzylidene derivatives were fully characterized by 1D and 2D NMR and, based on the unambiguous NOESY and coupling data (SI, Table S5) were straightforwardly assigned to specific diastereomeric acetals and from there connected to the specific stereoisomers of the corresponding diol. The *syn*-diol gave only a single benzylidene derivative I, while two were formed from the *anti*-isomer (II and III, SI, Table S5). Roughly, the relative abundances of the benzylidene derivatives were in accordance with their expected and calculated (MM+) relative stabilities; however, the numerical values seem to be under the influence of a kinetic factor since a much more significant predominance of the *syn* benzylidene derivative I should be expected (SI, Table S5). The conclusions coming from these experiments and the comparison of the shifts of the short diacetates were in agreement with the initial *syn*-assignment of the wax components.

Table 1

¹H (400 MHz) and ¹³C (100.6 MHz) NMR spectral data (in CDCl₃) of 1-phenylalkane-1,3-diyl diacetates (**syn-1a**, **2a-c**, **3a-b**, **4a-c**, **5a-b**, **6a-c**, and **7a-b**) from *P. veris* washings and their comparison with the NMR data of related compounds (**10** and **11**) from the literature (Niwa et al., 1987; Merad et al., 2017).

Position	δ_C	syn-1a, 2a-c, 3a-b, 4a-c, 5a-b, 6a-c, and 7a-b	10 ^a	11 ^b
			δ_H (<i>syn</i>)	δ_H (<i>anti</i>)
1	73.3	5.7854 (dd, <i>J</i> = 7.15, 6.70 Hz, 1H) ^c	5.79 (t, <i>J</i> = 7.0 Hz, 1H)	5.79 (dd, <i>J</i> = 10.1, 4.1 Hz, 1H)
2	40.4	2.0274 (ddd, <i>J</i> = -14.52, 6.70, 4.50 Hz, 1H) ^c 2.2322 (ddd, <i>J</i> = -14.52, 8.36, 7.15 Hz, 1H) ^c	/	1.98–2.08 (m, 1H) 2.12–2.21 (m, 1H)
3	71.2	4.7779 (dddd, <i>J</i> = 8.36, 6.30, 6.20, 4.50 Hz, 1H) ^c	4.85 (m, 1H)	5.14 (dddd, <i>J</i> = 8.7, 7.2, 5.2, 3.4 Hz, 1H)
4	34.4	1.5200 (ddd, <i>J</i> = -14.50, 7.00, 6.30 Hz, 1H) ^c 1.5290 (ddd, <i>J</i> = -14.50, 7.00, 6.20 Hz, 1H) ^c	/	/
5	25.7	1.25 (m, 2H)	/	/
6-(ω-4)	29.7	1.28 (m, overlapped H)	/	/
1'	140.0	/	/	/
2', 6'	127.8	7.34 (m, 2H) ^d	7.0–7.4	7.12–7.37 (10H)
3', 5'	128.2	7.35 (m, 2H) ^d	(10H)	
4'	126.7	7.35 (m, 1H) ^d		
1''	170.5	/	/	/
2''	21.2	2.0592 (s, 3H) ^c	2.01 (s, 3H)	/
1'''	170.1	/	/	/
2'''	21.3	1.9815 (s, 3H) ^c	1.95 (s, 3H)	/

/– data not available or not applicable.

^a (1*S*,3*S*)-1,5-diphenylpentane-1,3-diyl diacetate (**10**, *syn* isomer, Fig. 3, Niwa et al., 1987).

^b (1*S*,3*R*)-1,5-diphenylpentane-1,3-diyl dipropionate (**11**, *anti* isomer, Fig. 3, Merad et al., 2017).

^c Chemical shifts (4 decimal places) and coupling constants (two decimal places, and the sign) were determined based on spin simulation (Fig. 1) using Mestrelab Research S.L. (MestReNova) software package.

^d Chemical shifts were estimated based on the middle of the corresponding cross-peaks observed in the gHSQC spectrum.

With the *syn*- and *anti*-1-phenyl-1,3-butanediyl diacetates (**8a**) at hand (NMR data is given in the SI, Table S6), one could conclude that the difference in the GC retention indices of around 14 for these diastereoisomers could fall in the range of Δ RI between *iso*- and *anteiso*-regioisomers (ca. 8 units). Thus, it was necessary to exclude the possibility of misidentification of *syn-anti*-stereoisomers with *iso-anteiso*-regioisomers, or other combinations, especially since their MS data are uninformative in this respect. The most important verification of the non-existence of the *anti*-diastereoisomer came from NMR, since no traces of the signals that should correspond to this isomer could be located. However, due to the insensitivity of NMR in this sense, and due to the possible problems with the signal overlap, another synthetic endeavor was undertaken and three *syn-anti*-pairs of *n*-, *iso*- and *anteiso*-regioisomers (SI, chapters 2.3. and 2.4.) were prepared. A chain elongation of the available 1-phenylbutane-1,3-dione (**28a**) by a double deprotonation and subsequent alkylation with appropriate isomeric alkyl halides (SI, Figure S6) was opted for. The obtained **29a**, **29b**, and **29c** were, analogously to the short model compound **8a**, transformed first into longer-chain diols **13a**, **13b**, and **13c** (Figure S5, SI) and then into longer-chain diacetates **9a**, **9b**, and **9c** (Fig. 3). All of the prepared compounds were fully spectrally characterized, and their NMR shifts assigned (Tables S7 and S8, for diols, Tables S9 and S10, for diacetates, and Table S11 for diones, presented in the SI material). In the case of **9c** and **13c**, two pairs of *syn-anti*-stereoisomers were expected due to the existence of a third stereocenter, but these were not visible in the TIC

chromatograms, and did not display significantly different NMR shifts to be distinguished (SI, Tables S7 – S10). The NMR data of the synthesized compounds (**9a**, **9b**, **9c**, **29a**, **29b**, and **29c**) fully corresponded to the spectral data extracted from the NMRs of the fraction. Moreover, having ¹³C NMR data for both *syn*- and *anti*-isomers of diols, benzylidene derivatives, and diacetates, the generalization regarding the chemical shifts differentiation among such isomers (Hoffmann and Weidmann, 1985; Pelter et al., 1993) could now be tested. It is known that the sum of the ¹³C NMR chemical shifts of C-1 and C-3 carbons (chiral centers) of the *syn*-isomers are always higher than that of the *anti*-isomers. This proved to be correct for our compounds as well (SI, Table S12) and serves as another proof of the proposed stereostructures.

The final step in the corroboration of the structure and relative configuration of the diacetates, i.e., the connection of the non-functionalized chain termini with the functionalized chain-end, could now be performed. Only the most abundant diacetate (**4b**) displayed the M⁺ ion and was directly connected to the overall number of carbon atoms present in its chain (Figure S4-4, SI). For the rest of the diacetates, the length of the chain was inferred from the value of the ion corresponding to the loss of one acetic acid moiety which was prominent in all detected diacetates. A homologous series of compounds shows a quantitative structure-property regularity which is most evident in their GC retention data (Peng, 2000, 2010). A linear correlation between the increasing number of chain carbon atoms with the value of the retention index is expected within a single class of homologous compounds (Peng, 2000, 2010). Thus, one isomer, both in case of stereo- and regioisomerism, would belong to a single linear dependency representing the correlation between a structural parameter and the corresponding property. The RI data for the synthesized and natural diacetates within families of isomers to verify whether they belonged to the specific isomer group were then correlated. The obtained correlation equations, and their parameters, given in the SI material (Figure S7, SI), completely supported the existence of only *syn* stereoisomers in *P. veris* washings, but these were additionally separated into three regioisomeric classes, i. e. the ones differing in the branching of the other chain terminus. For all correlations, R² were found to be > 0.99 (Figure S7, SI), although unequal weighting of compounds, having drastically different number of carbon atoms in the chains, in the regression analysis should be kept in mind. In such a way the problem coming from the non-existence of M⁺ ions in the mass spectra of these compounds could also be remedied.

Hence, in this way we identified 16 completely new *syn*-1-phenylalkane-1,3-diyl diacetates (**syn-1a**, **2a-c**, **3a-b**, **4a-c**, **5a-b**, **6a-c**, and **7a-b**) having from 14 to 20 carbon atoms in the chains and distributed unevenly in *n*-, *iso*- and *anteiso*-series (SI, Table S3). Compounds with related structure were only once encountered in nature within lipids from sunflower pollen (*Helianthus annuus* L.) that was found to contain *n*-1-phenyl-1,3-diketones, and the related hydroxyketones and diols (Schulz et al., 2000). Not only that, up to now, 1-phenylalkane-1,3-diyl diacetates have never been previously detected, their uniqueness is even greater as they display a preference for *iso*-branched vs. *n*-counterparts: 1.8 to 1 ratio based on the total relative TIC-integral values.

2.2. 3-Oxo-1-phenylalkan-1-yl acetates

At first, the series of compounds **14a**, **15b**, **16a**, **17b-c**, **18a**, and **19b** (Fig. 4, and Figure S1, SI), with mass spectra displaying fragment ions at *m/z* 103 [PhCHCH]⁺, 131 [PhCHCHCO]⁺, and 146 [PhCHCHCOCH₃]⁺, appeared that they could represent 1-phenylalk-1-en-3-ones. However, the ¹H NMR spectrum of the fraction showed no signals for protons on double bonds. 3-Oxo-1-phenylalkan-1-yl acetates would also yield these fragment ions after the initial loss of acetic acid. An inspection of the 2D NMR spectra and a comparison of the available NMR data with the ones from the literature (compounds **20** and **21**, Fig. 4, Table 2, Xu and Yuan, 2005; Xu et al., 2016) were undertaken. The most helpful for elucidation purposes was the ¹H-¹H COSY spectrum (Fig. 4), as well as ¹H NMR spectral simulation (Fig. 2), which permitted us to verify the structure of

Table 2

^1H (400 MHz) and ^{13}C (100.6 MHz) NMR spectral data (in CDCl_3) of 3-oxo-1-phenylalkane-1-yl acetates (**14a**, **15b**, **16a**, **17b-c**, **18a**, and **19b**) from *P. veris* washings and the comparison of proton/carbon-13 signals with the ones of related compounds from the literature (**20** and **21**; Xu and Yuan, 2005; Xu et al., 2016).

Position	14a, 15b, 16a, 17b-c, 18a, and 19b		20 ^a	21 ^b	
	δ_{C}	δ_{H}	δ_{H}	δ_{C}	δ_{H}
1	71.7	6.1905 (dd, $J = 8.62, 5.10$ Hz, 1H) ^c	6.20 (dd, $J = 8.7, 4.8$ Hz, 1H)	70.7	6.25 (dd, $J = 8.1, 5.5$ Hz, 1H)
2	49.2	2.7927 (dd, $J = 16.40, 5.10$ Hz, 1H) ^c 3.0849 (dd, $J = 16.40, 8.62$ Hz, 1H) ^c	2.97 (dd, $J = 16.8, 4.8$ Hz, 1H)	48.5	2.78–3.15 (m, 2H)
3	206.7 ^d	/	/	206.2	/
4	43.9	2.42 (t, $J = 7.2$ Hz, 2H)	/	45.3	2.32–2.46 (m, 2H)
2', 6'	126.6 ^e	7.34 (m, 2H) ^e	7.26–7.36 (m, 5H)	/	/
3', 5'	128.2 ^e	7.35 (m, 2H) ^e	/	/	/
4'	127.7 ^e	7.35 (m, 1H) ^e	/	/	/
1''	170.5 ^e	/	/	169.7	/
2''	21.2 ^e	2.06 (s, 3H) ^e	/	21.0	2.07 (s, 3H)

/– data not available or not applicable.

^a Methyl 5-(butyryloxy)-3-oxo-5-phenylpentanoate (**20**, Fig. 4; Xu and Yuan, 2005).

^b 1-(4-Nitrophenyl)-3-oxohexyl acetate (**21**, Fig. 4; Xu et al., 2016).

^c Chemical shifts (4 decimal places) and coupling constants (two decimal places, and the sign) were determined based on spin simulation (Fig. 2) using Mestrelab Research S.L. (MestReNova) software package.

^d Signal assignment is based solely on the comparison with the literature data given in this Table.

^e Overlapped signals with those from compounds **1a**, **2a-c**, **3a-b**, **4a-c**, **5a-b**, **6a-c**, and **7a-b**.

the seven detected 3-oxo-1-phenylalkane-1-yl acetates, subdivided into three groups based on the *n*-, *iso*- and *anteiso*-nature of the other chain-end (**14a**, **15b**, **16a**, **17b-c**, **18a**, and **19b**, respectively, Fig. 4, and SI, Table S14). These compounds possessed the same numbers of carbon atoms in the side chains as the ones in the detected 1-phenylalkane-1, 3-diyl diacetates. To clarify and confirm the structure of 3-oxo-1-phenylalkane-1-yl acetates, 3-oxo-1-phenyltetradecyl and 1-oxo-1-phenylundecan-3-yl acetates were synthesized. Aldol reactions of the kinetic lithium enolate of 2-tridecanone and benzaldehyde, as well as of the lithium enolate of acetophenone and nonanal were performed to give 1-hydroxy-1-phenyltetradecan-3-one and 3-hydroxy-1-phenylundecan-1-one, respectively. Steglich esterification with acetic acid gave the target acetates (SI, chapter 2.6). The NMR data of 3-oxo-1-phenyltetradecyl acetate corresponded to the data that was obtained from the NMRs of the fraction. No evidence of the signals of 1-oxo-1-phenylalkane-3-yl acetates could be found in the NMRs of the fraction.

The product of aldol condensation, (*E*)-1-phenyltetradec-1-en-3-one, isolated from the first mentioned reaction mixture, along with 1-hydroxy-1-phenyltetradecan-3-one (**37a**), proved to be of importance for the interpretation of the GC-MS data. The peaks initially attributed to 3-oxo-1-phenylalkane-1-yl acetates observed in the TIC chromatograms of the fraction in fact corresponded to (*E*)-1-phenylalk-1-en-3-ones based on both their MS and RI data (SI, Figure S8; Table S13). It appears that 3-oxo-1-phenylalkane-1-yl acetates, present in the fraction, undergo complete elimination of acetic acid in the GC injector (at 250 °C). A similar behavior was observed for 1-hydroxy-1-phenylalkane-3-ones, losing a water molecule, making them impossible to detect by GC without silylation. It appears that the corresponding regioisomers of the acetates, 1-oxo-1-phenylalkane-3-yl acetates, also readily eliminate AcOH under GC conditions based on the conduct of 1-oxo-1-phenylundecan-3-yl acetate, while 3-hydroxy-1-phenylundecan-1-one did not undergo the loss of water under such conditions.

Only the sunflower pollen lipids were previously found to contain related wax constituents, 1-hydroxy-1-phenyl-3-hexadecanone and 1-hydroxy-1-phenyl-3-octadecanone (Schulz et al., 2000). These β -hydroxyketones possessed the same number of C-atoms in the side chains as the herein detected 3-oxo-1-phenyl-1-alkyl acetates, along

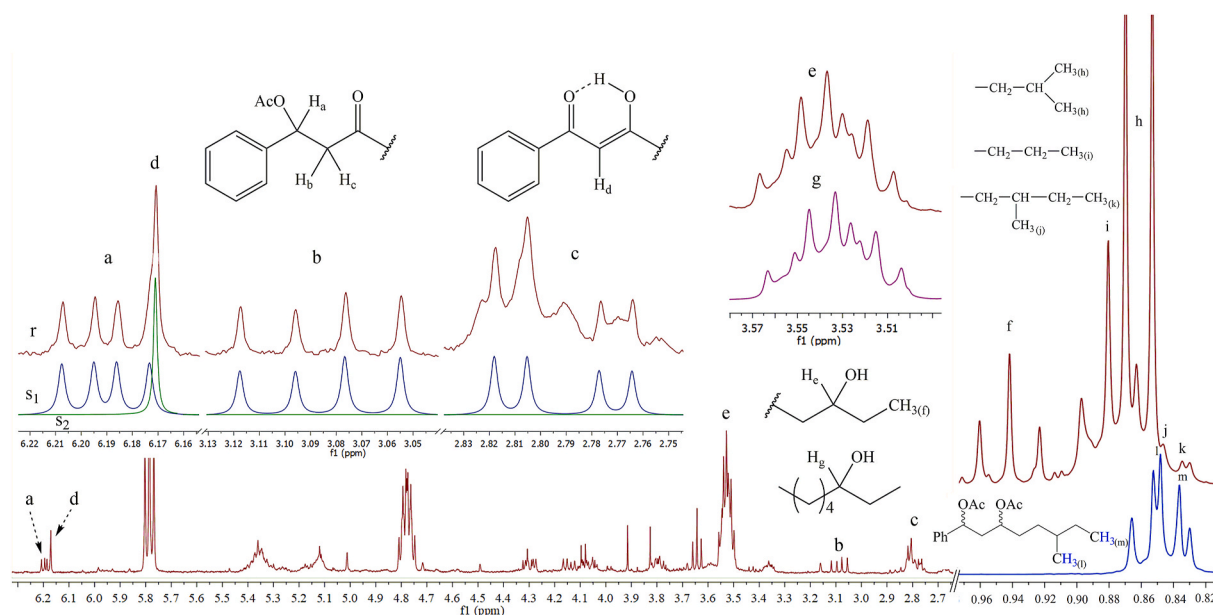
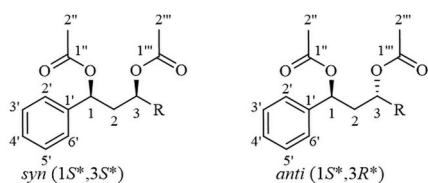


Fig. 2. ^1H NMR spectrum of a chromatographic fraction of *P. veris* aboveground wax with expansions (maroon trace) of signals belonging to 3-oxo-1-phenylalkane-1-yl acetates (**14a**, **15b**, **16a**, **17b-c**, **18a**, and **19b**, signals a-c), 1-phenylalkane-1,3-diones (**22a**, **23b-c**, **24a**, **25b-c**, **26a**, and **27b**, signal d), 3-alkanols (**49a**, **50a-b**, **51a-c**, **52a-c**, **53a-c**, **54a-c**, **55a**, **56a-c**, **57a**, **58a-b**, and **59a**, signals e and f), 3-octanol (signal g), chain termini (signals h-k) and 6-methyl-1-phenyloctane-1,3-diyl diacetate (**9c**, signals l and m). “s₁” and “s₂” are traces giving the simulated signals of these wax constituents, while “r” represents the corresponding experimental spectrum expansions.



	a (<i>n</i> -)	b (<i>iso</i> -)	c (<i>anteiso</i> -)
R			
n			
1	10 (0.9) ^x	/	/
2	11 (tr)	9 (4.1)	8 (tr)
3	12 (4.6)	10 (0.2)	/
4	13 (0.1)	11 (18.6)	10 (2.9)
5	14 (8.4)	12 (tr)	/
6	15 (0.8)	13 (2.8)	12 (0.6)
7	16 (tr)	14 (tr)	/
8	0	/	/
9	5	3	2

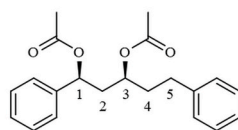
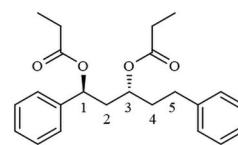
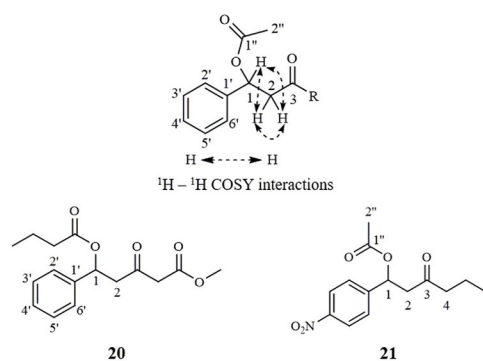
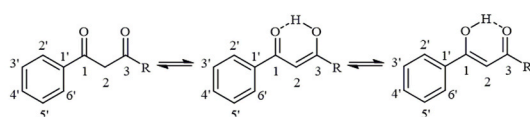
**10**(1*S*,3*S*)-1,5-diphenylpentane-1,3-diyl diacetate (*syn* isomer) (1*S*,3*R*)-1,5-diphenylpentane-1,3-diyl dipropionate (*anti* isomer)**11**

Fig. 3. Structures of 1-phenylalkane-1,3-diyl diacetates from *P. veris* washings (**syn-1a**, **2a-c**, **3a-b**, **4a-c**, **5a-b**, **6a-c**, and **7a-b**) and the ones obtained by synthesis (**syn**- and **anti-8a** and **9a-c**), and compounds (**10** and **11**) from the literature (Niwa et al., 1987; Merad et al., 2017) used for stereochemistry assignment; ^x – the number in brackets represents the percentage content of the compound in the fraction of *P. veris* washings (tr, trace, <0.05%).

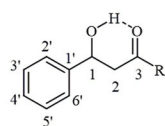
A**20****21**

	a (<i>n</i> -)	b (<i>iso</i> -)	c (<i>anteiso</i> -)
R			
n			
14	10 (tr) ^w	/	/
15	/	9 (0.2) ^w	/
16	12 (0.7) ^w	/	/
17	/	11 (1.6) ^w	10 (0.1) ^w
18	14 (0.7) ^w	/	/
19	/	13 (0.2) ^w	/

Fig. 4. Structures of: **A** – 3-oxo-1-phenylalkane-1-yl acetates (**14a**, **15b**, **16a**, **17b-c**, **18a**, and **19b**), compounds (methyl 5-(butyryloxy)-3-oxo-5-phenylpentanoate (**20**) and 1-(4-nitrophenyl)-3-oxohexyl acetate (**21**)) from the literature (Xu and Yuan, 2005; Xu et al., 2016) used for the structural elucidation and synthesized hydroxyketone **14a**, **B** – 1-phenylalkane-1,3-diones (**22a**, **23b-c**, **24a**, **25b-c**, **26a**, and **27b**), the commercial diketone (**28a**), and the synthesized diketones (**29a-c**), **C** – 1-hydroxy-1-phenylalkane-3-ones (**30b**, **31a-b**, **32a-b**, **33a**, **34b-c**, **35a**, and **36b**) and the synthesized hydroxyketone (**37a**), from *P. veris* washings; ^w – the number in brackets represents the percentage content of the compound in the fraction of *P. veris* washings (tr, trace, <0.05%), ^x – the number in brackets represent the percentage content of the enol in the tautomeric equilibrium, ^y – compounds detected in *P. veris* washings by TMS derivatization, ^z – compound obtained by synthesis: 1-hydroxy-1-phenyltetradecan-3-one (**37a**).

B

	a (<i>n</i> -)	b (<i>iso</i> -)	c (<i>anteiso</i> -)
R			
n			
22	20 (tr) ^w	/	/
23	/	19 (0.4) ^w	18 (0.1) ^w
24	22 (0.1) ^w	/	/
25	/	21 (0.5) ^w	20 (0.2) ^w
26	24 (tr) ^w	/	/
27	/	23 (tr) ^w	/
28	0 (89) ^x	/	/
29	5 (96) ^x	3 (97) ^x	2 (92) ^x

C

	a (<i>n</i> -)	b (<i>iso</i> -)	c (<i>anteiso</i> -)
R			
n			
30	/	9 ^y	/
31	13 ^y	11 ^y	/
32	21 ^y	19 ^y	/
33	22 ^y	/	/
34	/	21 ^y	20 ^y
35	24 ^y	/	/
36	/	23 ^y	/
37	10 ^z	/	/

with an additional dinor homolog (C₁₄). Not only is this the first report of 3-oxo-1-phenyl-1-alkyl acetates, but the ratio between the *iso*-branched and *n*-isomers: 1 to 0.7, based on the relative TIC-integral values, is unique as well.

2.3. 1-Phenylalkane-1,3-diones

Having identified the two previous classes of wax constituents, one would expect to find the corresponding fully oxidized counterparts, i.e. to detect 1-phenylalkane-1,3-diones. As members of this homologous series (having C₁₂, C₁₅–C₂₂ *n*-chains) have been identified in the pollen of *H. annuus* (Schulz et al., 2000), and the MS of C₁₆ and C₁₈ homologs published therein, it was possible to search the TIC for ion currents characteristic of the diketones (*m/z* 162, SI, Figure S1). Indeed, the β-diketones were present in the fraction, however, surprisingly, judging from the retention times, the lengths of the side chains were significantly longer than those of the previously reported from *H. annuus*, as well as from the closely related 1-phenylalkane-1,3-diyl diacetates and 3-oxo-1-phenylalkane-1-yl acetates (SI, Figure S1). Thus, this implies that they have not formed from diacetates (*syn*-1a, 2a-c, 3a-b, 4a-c, 5a-b, 6a-c, and 7a-b) or ketoacetates (14a, 15b, 16a, 17b-c, 18a, and 19b) in an (envisagable) artefactual manner (hydrolysis and autooxidation).

The detected 1-phenylalkane-1,3-diones displayed the following characteristic mass fragmentation pattern: *m/z* 105 [PhCO]⁺, *m/z* 120 [Ph(CO)CH₃]⁺, *m/z* 147 [Ph(CO)CH₂(CO)]⁺, and *m/z* 162 [Ph(CO)CH₂(CO)CH₃]⁺. The molecular and [M – 18]⁺ ions were clearly noticeable in the MSes (SI, Table S15; Figure S9-1 – 9-4), allowing the total number of C-atoms in the chains to be easily deduced (C₂₄–C₂₉); however, the main challenge here was to determine the RI values of 1-phenyl-1,3-alkanediones. For our usual GC-MS temperature-programmed runs (70(0')/5 °C/min/315(isothermal 30'), He flow 1.0 ml/min) for the analysis of wax constituents, the linear programing ends at ca. 49 min, and the majority of the detected diketones eluted after this limit hampering the usual calculation of RIs (Van Den Dool and Kratz, 1963). The precise values of RIs are essential for the discrimination of the branched members of the series. Therefore, the fraction was re-analyzed using another longer GC-temperature program (200(0') 1 °C/min/315(isothermal 30'), He flow 1.5 ml/min), and all the detected compounds were now located in the linear part of the program. As mentioned above, the three (*n*-, *iso*- and *anteiso*-) isomers of C₉ β-diketones (29a, 29b, and 29c, Fig. 4 and SI, Figure S6) were available to us via synthesis.

Analysis of the NMR spectra of the synthesized β-diketones (29a-c, SI, chapter 2.3.) and 28a pointed to the dominant existence (>89%) of the keto-enol tautomers (Fig. 4), while the relative share of the diketone form expectedly decreased (Masur et al., 1987) with the length of the side chain. The GC-MS chromatograms of the commercial and synthetic samples did not show a separation of the tautomeric forms, but a significant broadening of the target peak (in the same cases going up to 5 RI units). This broadening was accompanied by a change in the intensities of the detected ions in the mass scans throughout the peaks, a characteristic of the two tautomeric forms (Masur et al., 1987). Thus, it might be that the tautomeric forms of the herein analyzed specific β-diketones are highly similar in retention behavior, as also previously published (Masur et al., 1987). The chromatograms of the analyzed wax fraction did not show indications of separated peaks of the diketone forms (the MS corresponded better to the keto-enol form), as anticipated based on their very low abundance, which is the consequence of both their expected low percentage in the tautomeric equilibrium and their overall low abundance in the fraction. The NMR of the fraction was, unfortunately, of little help at this point as the signal of the C-2 methylene group of the diketone form was probably hidden within multiple other signals around 4 ppm. The singlet corresponding to the C-2 of the keto-enol form was readily detected at 6.18 ppm (s, 1H), attached to a carbon resonating at 95.8 ppm, which is in accordance with the NMR data of the reference compounds (Figs. 2 and 4, and SI, Table S11). Having cleared the

situation regarding the possible presence of peaks coming from the diketone forms, the determined RI values of eight detected 1-phenylalkane-1,3-diones straightforwardly differentiated the *n*-, *iso*-, and *anteiso*-series (SI, Figures S1 – S2, and S10, and Table S2). Thus, in this way 8 new 1-phenylalkane-1,3-diones (possessing 24–29 C-atoms in the chains), more precisely their enol-keto forms, were identified (Fig. 4, and SI, Table S16). Once again it should be stressed that this is the first detection of branched members of this class of compounds.

2.4. 1-Hydroxy-1-phenylalkane-3-ones

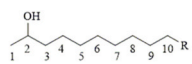
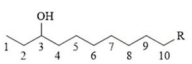
Long-chained 1-hydroxy-1-phenylalkane-3-ones were undetectable in the TIC chromatogram of the underivatized fraction due to the loss of H₂O under GC conditions as specified above; however, silylation disclosed 10 1-hydroxy-1-phenylalkane-3-ones (30b, 31a-b, 32a-b, 33a, 34b-c, 35a, and 36b, Fig. 4 and the SI, chapter 2.5, and Table S17). 1-Hydroxy-1-phenyltetradecan-3-one (37a) was synthesized as mentioned above, and silylated to confirm the tentative identifications (SI, chapters 2.5. and 2.6.). The matching of MS data and RI correlations for the silylated derivatives allowed the identification of 1-hydroxy-1-phenylalkane-3-ones having 15, 17, and 25–29 C-atoms in the chains (SI, Figure S11 and Table S17). Such compounds, but of differing chain lengths, were only once found in nature within lipids from sunflower pollen (*H. annuus*, Schulz et al., 2000), hence all identified here represent unreported natural compounds. Based on the number of C-atoms in the chains of 1-hydroxy-1-phenylalkane-3-ones, it appears that they may have two (biosynthetic) origins: one related to 1-phenylalkane-1,3-diones (homologs with 25–29 C-atoms in the chains), or another related to 3-oxo-1-phenylalkane-1-yl acetates (compounds with 15 and 17 C-atoms in the chains).

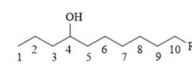
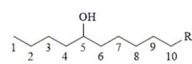
2.5. Secondary alcohols (2- to 10-alkanols)

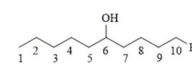
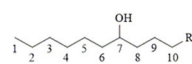
An observed series of peaks in the TIC, displaying a base peak at *m/z* 59 [CH₃CH₂CHOH]⁺, an evident loss of water [M – 18]⁺, and the loss of an ethyl group [M – 29]⁺ (SI, Figures S12-1 – S12-2 and Table S18), pointed to the presence of long-chain 3-alkanols. The ¹H NMR spectrum of the fraction contained a relatively complex multiplet at 3.52 ppm (a broadened pseudo tt, *J* ≈ 7.3, 4.7 Hz, 1H, CH₃CH₂CH(OH)CH₂, Table 3 and Fig. 2), corresponding to a significant share of the total integrated ¹H NMR areas, suggesting the presence of an alcoholic group somewhere in the interior of the chains (1- or 2-alkanols are easily discernible based on the coupling pattern of the corresponding carbinol hydrogen). 3-Alkanols (Fig. 2) and secondary alcohols other than 2-alkanols fit this criterium. To confirm this, the NMR spectra of commercially available 3-octanol were recorded (SI, Table S19). It displayed an identical carbinol-H signal of interest (Fig. 2, g and e), and it is now possible to explain the complexity (broadening and appearance of additional coupling) of the multiplet as arising from the virtual coupling caused by mutually strongly coupled methylene groups in the vicinity of the alcohol chiral

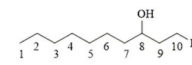
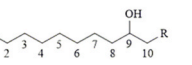
Table 3
¹H (400 MHz) and ¹³C (100.6 MHz) NMR spectral data (in CDCl₃) of 3-alkanols (49a, 50a-b, 51a-c, 52a-c, 53a-c, 54a-c, 55a, 56a-c, 57a, 58a-b, and 59a) and 2-alkanols (38a, 39a-c, 40a-b, 41a-c, 42a-b, 43a-c, 44a, 45a-c, and 46a) from *P. veris* washings.

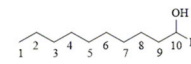
Position	δ _C	δ _H
3-alkanols		
1	9.9	0.94 (t, <i>J</i> = 7.5 Hz, 3H)
2	34.1	1.52 (m, 2H, overlapped with the <i>anteiso</i> -chain-end protons)
3	73.4	3.52 (broad pseudo tt, <i>J</i> ≈ 7.3, 4.7 Hz, 1H)
4	37.0	1.45 (m, 2H)
2-alkanols		
1	23.6	1.19 (d, <i>J</i> = 6.2 Hz, 3H)
2	68.3	3.79 (m, 1H)
3	39.2	1.40 (m, 2H)

							
R		a (<i>n</i> -)	b (<i>iso</i> -)	c (<i>anteiso</i> -)	a (<i>n</i> -)	b (<i>iso</i> -)	c (<i>anteiso</i> -)
		n					
38		12 (2.6) ^x	/	/	49	10 (tr)	/
39		13 (1.5)	11 (13.8)	10 (1.4)	50	11 (0.6)	9 (0.4)
40		14 (11.3)	12 (4.0)	/	51	12 (16.5)	10 (0.9)
41		15 (0.8)	13 (17.0)	12 (6.5)	52	13 (1.8)	11 (35.8)
42		16 (7.2)	14 (2.0)	/	53	14 (1.1)	12 (9.7)
43		17 (1.3)	15 (4.5)	14 (2.8)	54	15 (0.4)	13 (9.3)
44		18 (3.9)	/	/	55	16 (3.3)	/
45		19 (0.4)	17 (0.5)	16 (0.2)	56	17 (0.2)	15 (1.3)
46		20 (0.3)	/	/	57	18 (0.7)	/
47		1	/	/	58	19 (0.2)	17 (0.2)
48		4	/	/	59	20 (0.3)	/
		n					
60		1	/	/	60	1	/
61		4	/	/	61	4	/

							
R		a (<i>n</i> -)	b (<i>iso</i> -)	c (<i>anteiso</i> -)	a (<i>n</i> -)	b (<i>iso</i> -)	c (<i>anteiso</i> -)
		n					
62		/	11 (23.5)	10 (10.0)	71	/	11 (0.7)
63		/	12 (2.3)	/	72	/	12 (5.6)
64		/	13 (3.9)	/	73	/	14 (4.2)
65		/	15 (0.5)	/	74	/	16 (3.4)
66		/	16 (1.4)	/	75	1	/
67		/	17 (1.5)	/	76	4	/
68		/	18 (0.6)	/			
69		1	/	/			
70		4	/	/			

							
R		a (<i>n</i> -)	b (<i>iso</i> -)	c (<i>anteiso</i> -)	a (<i>n</i> -)	b (<i>iso</i> -)	c (<i>anteiso</i> -)
		n					
77		/	10 (1.6)	/	84	10 (1.7)	8 (0.8)
78		/	14 (7.9)	/	85	/	10 (76.5)
79		17 (0.8)	/	/	86	/	12 (4.9)
80		18 (3.1)	16 (0.1)	/	87	/	14 (9.3)
81		/	18 (2.2)	/	88	4	/
82		1	/	/			
83		4	/	/			

							
R		a (<i>n</i> -)	b (<i>iso</i> -)	c (<i>anteiso</i> -)	a (<i>n</i> -)	b (<i>iso</i> -)	c (<i>anteiso</i> -)
		n					
89		10 (1.8)	/	/	95	10 (0.5)	/
90		12 (1.8)	10 (32.8)	/	96	12 (1.7)	10 (18.1)
91		/	12 (13.3)	/	97	/	12 (42.3)
92		/	14 (13.6)	/	98	/	14 (7.9)
93		/	16 (9.7)	/	99	/	16 (9.0)
94		4	/	/			

				
R		a (<i>n</i> -)	b (<i>iso</i> -)	c (<i>anteiso</i> -)
		n		
100		/	12 (5.9)	/
101		/	16 (53.9)	/

(caption on next column)

Fig. 5. Structures of *sec*-alkanols identified after silylation (2-alkanols: **38a**, **39a-c**, **40a-b**, **41a-c**, **42a-b**, **43a-c**, **44a**, **45a-c**, and **46a**; 3-alkanols: **49a**, **50a-b**, **51a-c**, **52a-c**, **53a-c**, **54a-c**, **55a**, **56a-c**, **57a**, **58a-b**, and **59a**; 4-alkanols: **62b-c**, and **63–68b**; 5-alkanols: **71–74b**; 6-alkanols: **77–78b**, **79a**, **80a-b**, and **81b**; 7-alkanols: **84a-b**, and **85–87b**; 8-alkanols: **89a**, **90a-b**, and **91–93b**; 9-alkanols: **95a**, **96a-b**, and **97–99b**; 10-alkanols: **100–101b**) of *P. veris* washings fraction and the TMS derivatives of synthetic *sec*-alkanols (2-alkanols: **47–48a**; 3-alkanols: **60–61a**; 4-alkanols: **69–70a**; 5-alkanols: **75–76a**; 6-alkanols: **82–83a**; 7-alkanol: **88a**; 8-alkanol: **94a**); ^x – the number in brackets (tr, trace, <0.05%) represents the percentage content of the compound within a group of homologs with *n*-, *iso*- and *anteiso*-chains with a single specific position of the OH group, which was obtained by integration of partial ions current chromatograms as detailed in the SI file (Table S21). Thus, the percentages are not comparable across different classes of alcohols (for example, 3-alkanols and 4-alkanols, etc.).

center and the majority of the remaining of CH₂ groups in the chain, and possibly due to the presence of other secondary alcohols. Judging from the regularities in their retention data (SI, Table S20), ten 3-alkanols (**50b**, **51a**, **52b-c**, **53a**, **54b-c**, **55a**, and **56b-c**) could be positively identified, none of which were previously detected in any samples of natural origin, having from 22 to 28 carbon atoms in the chains and distributed unevenly among the *n*-, *iso*-, and *anteiso*-series (Fig. 5 and SI, Table S20). Again, the *iso*-series dominated with C₂₄ as the most abundant contributor. Until now, only 3-tricosanol has been mentioned in the literature, and quite conveniently, its mass spectrum and retention index (on SE30) are available (Streibl and Stránský, 1972; Ubik et al., 1974), which matched nicely with our data. The other nine detected 3-alkanols are reported here for the first time.

To further confirm the presence of 3-alkanols, and possibly the presence of some other alkanols, the fraction was silylated. After derivatization, the characteristic mass fragmentation of TMS-derivatives (Harvey and Vouros, 2019) and regularities in RI values (SI, Figures S18 – S21 and Table S20 and S21) enabled not only the detection of additional 3-alkanols but led to the identification of in total 79 *sec*-alcohols with the position of the hydroxyl group varying from 2 to 10, having *n*-, *iso*-, and *anteiso*-chain termini (2-alkanols: **38a**, **39a-c**, **40a-b**, **41a-c**, **42a-b**, **43a-c**, **44a**, **45a-c**, and **46a**; 3-alkanols: **49a**, **50a-b**, **51a-c**, **52a-c**, **53a-c**, **54a-c**, **55a**, **56a-c**, **57a**, **58a-b**, and **59a**; 4-alkanols: **62b-c**, and **63–68b**; 5-alkanols: **71–74b**; 6-alkanols: **77–78b**, **79a**, **80a-b**, and **81b**; 7-alkanols: **84a-b**, and **85–87b**; 8-alkanols: **89a**, **90a-b**, and **91–93b**; 9-alkanols: **95a**, **96a-b**, and **97–99b**; 10-alkanols: **100–101b**, Fig. 5, and SI, Figure S13). GC-MS analysis of the silylated mixtures of synthetic *sec*-alcohols (2-dodecanol, 3-dodecanol, 4-dodecanol, 5-dodecanol and 6-dodecanol, and 2-pentadecanol, 3-pentadecanol, 4-pentadecanol, 5-pentadecanol, 6-pentadecanol, 7-pentadecanol and 8-pentadecanol) confirmed the identification (SI, Table S1 and Figures S14-1 – S14-5, S15, and S16). *sec*-Alcohols were obtained by unselective hydroxylation of *n*-dodecane and *n*-pentadecane using an *in situ* prepared H₂O₂-CF₃COOH (SI, chapter 2.7., Deno et al., 1977). The ¹H NMR spectrum contained the evidence (3.79 ppm, CH₃CH(OH)CH₂) for the presence of 2-alkanols, confirmed by the analogous signal of synthetic 2-tridecanol (SI, Figure S17). The corresponding -CH₂CH(OH)CH₂- signals from other *sec*-alcohols, expected to be of low intensity based on GC-MS, are most probably buried under the signal for 3-alkanols (3.49–3.56 ppm).

Out of the 79 identified *sec*-alcohols (with 21–31 C-atoms, Fig. 5, and SI, Table S21), 66 are unreported from the samples of natural origin. Among them, the normal-chained isomers of 7-, 8-, and 9-alkanols (and additional 3-alkanols with 21, 22, 24, 26, 28–31 C-atoms), as well as all branched (*iso*- and *anteiso*-) 2-, 3-, 4-, 5-, 6-, 7-, 8-, 9- and 10-alkanols are unreported natural products. The literature mentioning some of the alcohols is summarized in the SI (Table S22). The carbon-backbone of the identified *sec*-alcohols matches that of the wax alkanes previously reported from *P. veris* (Živković et al., 2016). Again, in accordance with the abovementioned wax compound series, the branched chains were

more abundant than the normal chained counterparts (Fig. 4, and SI, Table S21). It was not possible to perform an exact comparison of OH-positional isomer quantities within the fraction due to severe GC-peak overlap of the TMS derivatives of the alcohols; the percentage content of the compound within a group of homologs with *n*-, *iso*- and *anteiso*-chains with a single specific position of the OH group was evaluated (Fig. 4, and SI, Table S21) by the integration of partial ions current chromatograms. Only roughly, one might speculate that the possible MAH enzyme responsible for the hydroxylation of long-chain alkanes has a preference for position 3 over positions 2 and 4, while all other positions were much less frequently hydroxylated. Since no replicates were performed, this MAH preference should be taken with caution; however, it is known that MAH1 has a preference for positions 13 to 15 (central CH₂ group) in *Arabidopsis thaliana* (Wen and Jetter, 2009).

2.6. Fatty acids

The TIC chromatogram of the underivatized fraction displayed abundant and tailing ion currents with *m/z* values corresponding to a series of [HOOC(CH₂)_n]⁺ ions, accompanied by *m/z* 60, most probably originating from free fatty acids (FAs) present in the fraction. This was supported by the detected signal at δ 178.5 in the ¹³C NMR spectrum (SI, Figure S3), assignable to a carboxylic group (Pretsch et al., 2009). At first, it was odd that fatty acids co-eluted with secondary alcohols, diesters, diketones, etc., but this was straightforwardly verified to be true by a TLC analysis of commercially available long-chain alcohols and acids: 1-hexadecanol (spot 1), 1-octadecanol (spot 2), octadecanoic acid (spot 3) and docosanoic acid (spot 4), and the fraction (spot F) (SI, Figure S22). On silica gel, palmityl and stearyl alcohols were more polar (lower R_f) than stearic and behenic acids, while the acids had R_f values similar to that of the herein analyzed fraction.

The fraction was treated with CH₂N₂ (Ilic-Tomic et al., 2015), prior to silylation, to convert FAs to their methyl esters (SI, Figure S23) and reanalyzed. The obtained TIC chromatogram showed a plethora of non-tailing peaks with the characteristic mass fragmentation pattern of methyl esters which allowed both qualitative and quantitative analyses (by GC-MS) of these FAs via their methyl esters (SI, Table S23). The identification of saturated normal chain and branched fatty acids was based on a combination of data coming from the mass spectra and gas chromatographic retention behavior of the corresponding methyl esters and the NMR data of the chromatographic fraction. Methylene protons, assigned by the observed long-range interactions with the carboxylic

carbon in gHMBC, in the α- and β-positions appeared as a triplet at 2.36 (*J* = 7.5 Hz) and a pentet 1.65 ppm (*J* = 7.5 Hz; SI, Table S24). The identities of the majority of the 24 detected normal chain acid methyl esters (C₁₄, C₁₆–C₃₈, SI, Table S23) were corroborated by comparing their retention times with those from an analysis, under identical conditions on the same instrument, of a mixture of either commercially available fatty acid methyl esters or those obtained by methanolysis of beeswax (from C₁₄ up to C₃₂).

In total, 77 detected methyl esters formed five series based on the regularities in values of their RIs, one already identified as methyl esters of long-chain *n*-fatty acids (SI, Figure S26). The other four represented isomers of this series, displaying the same molecular weight but lower RI values. Among them the retention behavior of two series corresponded well to the *iso*- and *anteiso*-series (SI, Figure S26), while the two remaining series eluted even faster, suggesting that the branching is closer to the functionalized chain terminus (Kubinec et al., 2011). This was confirmed by observing three- and two-bond ¹³C–¹H couplings of the carbonyls in the gHMBC spectrum (181.8 ppm with H-2, and 177.9 ppm with Me-2', respectively (Fig. 6 and SI, Figure S3)), with chemical shifts of the carbonyls expected for 2- and 3-methylalkanoic acids (Couperus et al., 1978; Ejchart, 1981; Pretsch et al., 2009). Supporting the α- and β-branching were the prominent ions at *m/z* 88 and 101, (SI, Figure S23 – S25), arising from a Mc Lafferty rearrangement and the α-fragmentation at the branch, respectively (Apon and Nicolaides, 1975). To strengthen the identification of 2-methyl- and 3-methylalkanoic acids, the commercially available 2-methyl- and 3-methylhexanoic acids were fully NMR characterized (SI, Table S19), since, usually, only ¹³C NMR signals are reported (Couperus et al., 1978; Ejchart, 1981), and no ¹H NMR data are given. The assigned data corresponded to that from the NMRs of the fraction (SI, Table S19). The possible existence of two branches, for example an α,(ω-1)-dimethyl fatty acid, was clearly eliminated by the excellent correspondence between the equivalent chain lengths (Kubinec et al., 2011) and our own retention indices for the five isomeric methyl esters of C₂₁ and C₂₂ acids (SI, Figure S26). Unequivocal proof of the identities of 2-methylalkanoic acids was obtained by GC-MS co-injection experiments of synthetic methyl 2-methylhexadecanoate, methyl 2-methyloctadecanoate, and methyl 2-methyldocosanoate prepared by methylation of the corresponding lithium enolates of the appropriate methyl esters (SI, chapter 2.8.). In the case of 3-methylalkanoic acids, the standards were synthesized by a four-step sequence-aldol addition of lithium enolates of ethyl acetate to an appropriate 2-alkane, followed by dehydration to α,β-unsaturated esters, their

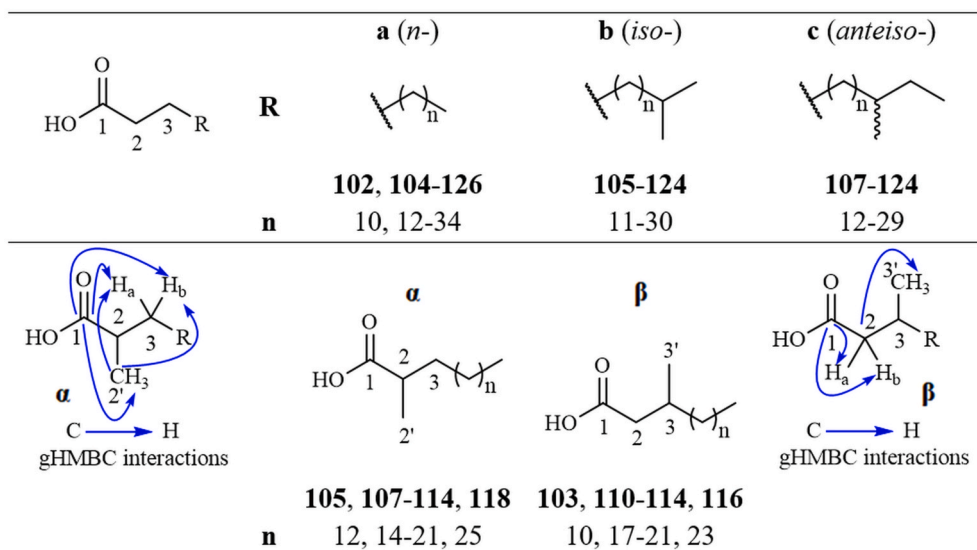


Fig. 6. Structures of free long-chain acids (normal-chain: 102a and 104–126a; *iso*-chain: 105–124b; *anteiso*-chain: 107–124c; 2-methyl: 105α, 108–114α and 118α; 3-methyl: 110–114β and 116β) from *P. veris* washings and the ones obtained by synthesis (105α, 107α, 111α, and 103β).

hydrogenation and methanolysis (SI, chapter 2.9).

In this way, 77 methyl esters of saturated normal and branched (2-methyl, 3-methyl, *iso*- and *anteiso*-) fatty acids (Fig. 6 and SI, Figure S27; Table S23) were positively identified, and their quantity determined (μg per mg of the fraction) as previously published (Ilic-Tomic et al., 2015). Among them, 32-methyltritriacontanoic, 33-methyltetraatriacontanoic, 34-methylpentatriacontanoic, 33-methylpentatriacontanoic, 2-methylpentacosanoic acid, and all detected 3-methyl substituted fatty acids (3-methylheneicosanoic, 3-methyldocosanoic, 3-methyltricosanoic, 3-methyltetracosanoic, 3-methylpentacosanoic, and 3-methylheptacosanoic acids) are new natural products. Erroneously, SciFinder® links 3-methyldocosanoic, 3-methyltetracosanoic, and 3-methylheptacosanoic acids with two studies (Rezanka, 1992; Bos et al., 2012), which do not contain any data related to these acids. 2-Methylheneicosanoic, 2-methyldocosanoic, and 2-methyltricosanoic acids have never previously been detected as free acids but only bound in phospholipids (Siljeström et al., 2017). Interestingly, 3-methylheneicosanoic acid was found to be active against mosquito larvae (Hwang et al., 1978). A summary of the literature dealing with some of the identified 2-methylalkanoic acids is provided in the SI (Table S25).

Thus, this is the first report of such long-chain 2-methyl- and 3-methylalkanoic acids (Fig. 6) in the Plant Kingdom. Biosynthetically speaking, the 2-methyl and 3-methylalkanoic acids might not originate from the same pathway as *iso*- and *anteiso*-branched fatty acids (Kunst et al., 2006). One could speculate that these were formed from the corresponding *iso*- and *anteiso*-alkanes by oxidation of the appropriate methyl groups, especially as this type of branching was found to be quite abundant in all classes of the wax *Primula* metabolites detected. One would, then, expect to find 2-ethylalkanoic acids, coming from the oxidation of the methyl branch in *anteiso*-alkanes, however, these were not detected in this fraction or any other, either due to the inefficiency of such oxidation and/or their exceedingly low relative amount. Alternatively, the biosynthesis of branched-chain FAs might involve *S*-adenosyl methionine-dependent methylation at the double bond of monoenoic acids. Subsequently, the resulting product is reduced to methyl compounds with NADPH as the cofactor (Buist, 2007). The third possibility is the known reaction of acetyl-CoA carboxylase on propionyl-CoA. Methylmalonyl-CoA is then incorporated into FAs by the fatty acid synthase. A consequence of this mechanism is that the methyl groups are all in the even-numbered positions of the given FAs. Further, the 3-methylalkanoic acids can be shortened by one methylene group by α -decarboxylation to form 2-methylalkanoic acids.

2.7. Quantification of classes of wax constituents

The relative amounts of some of the identified compound classes could be inferred from the ^1H NMR profile of the fraction based on characteristic proton resonances, non-overlapped with other signals (Figs. 1 and 2). Thus, the ratio of *syn*-1-phenylalkane-1,3-diyl diacetates, 3-oxo-1-phenyl-1-alkyl acetates, 1-phenyl-1,3-alkanediones, and 3-alkanols (together with other *sec*-alcohols) based on qNMR equals 1 : 0.08: 0.03 : 0.57, while based on TIC integration (the methylated sample), this ratio is 1 : 0.08: 0.04 : 1.23, respectively. The discrepancy in the relative content of 3-alkanols is the consequence of the different sensitivity of the MS detector to aromatic compounds and completely aliphatic ones. Having the quantity of fatty acids already determined as stated above, and if one neglects the surface of the flowers, then calculated per cm^2 of the leaf surface, the total amounts in μg of the following classes of wax constituents present in this fraction are 0.49, 0.04, 0.02, 0.25, and 0.93 for *syn*-1-phenylalkane-1,3-diyl diacetates, 3-oxo-1-phenylalk-1-yl acetates, 1-phenylalkane-1,3-diones, 3-alkanols, and fatty acids, respectively.

3. Conclusions

This work provides the results of the very first study of non-flavonoid

constituents of surface waxes of *P. veris*. Herein, *syn*-1-phenylalkane-1,3-diyl diacetates, 3-oxo-1-phenylalkane-1-yl acetates, 1-phenylalkane-1,3-diones, 1-hydroxy-1-phenylalkane-3-ones, *sec*-alcohols (2- to 10-alkanols), and branched fatty acids, among which 118 unreported (natural) compounds, are described. It was revealed that this species produces, alongside normal-chain homologs, unusually high amounts of branched (*iso*- and *anteiso*-) isomers, together with exceedingly rare 2-methylalkanoic and 3-methylalkanoic acids. The identity of the wax constituents was unambiguously confirmed by a combination approach: synthesis of the model compounds of possible (stereo/regio)isomers, CH_2N_2 derivatization and silylation of the sample, 1D and 2D NMR analyses of the sample, interpretation of the mass spectral data, and modelling of RI data. This approach made it possible to overcome the lack of commercial standards, and RI data in the literature, and non-separation of the members of homologous series by liquid chromatographies and the low available amount of the sample.

Hence, in this way, 16 unreported *syn*-1-phenylalkane-1,3-diyl diacetates, 7 unreported 3-oxo-1-phenylalkane-1-yl acetates, 8 unreported 1-phenylalkane-1,3-diones, 10 unreported 1-hydroxy-1-phenylalkane-3-ones, and 79 *sec*-alcohols (2- to 10-alkanols, among which 66 are unreported natural products), subdivided into three groups based on the *n*-, *iso*- and *anteiso*-nature of the other chain-end, were identified, none of which were previously detected in the samples of natural origin. Also, 77 methyl esters of saturated normal and branched (2-methyl, 3-methyl, *iso*- and *anteiso*-) fatty acids were positively identified. Among them, 11 branched acids represent unreported natural products and a number of others are reported on for the first time in the Plant Kingdom. It is important to stress that, with the exception of the identified fatty acids, all other classes of the wax constituents displayed predominance (>60%) of *iso*- and *anteiso*-regioisomers compared to the normal counterparts. The total relative amount of branched (*iso*-, *anteiso*-, 2-methyl-, and 3-methyl-) fatty acids was also a significant one (>40%). Such high abundance of the branched wax constituents suggests a possible ecological role, and a diversification of the biosynthesis of wax components in *P. veris* compared to other plant taxa. The existence of 2- and 3-methylalkanoic acids also hints at another biosynthetic pathway to fatty acids to be operational.

4. Experimental

4.1. General experimental procedures

All commercially available chemicals (Aldrich, USA; Merck, Germany; Acros Organics, Belgium) were used without further purification except that solvents were freshly distilled prior to use. Chromatographic separations were carried out using silica gel 60 (particle size distribution 35–70 μm) purchased from Acros Organics (Geel, Belgium). TLC experiments were performed on alumina-backed silica gel 40 F₂₅₄ plates (MACHEREY-NAGEL GmbH & Co. KG, Düren, Germany). The spots on TLC were visualized by UV light (254 nm) and by spraying with 50% (v/v) aqueous H_2SO_4 or phosphomolybdic acid (12 g) in EtOH (250 ml) followed by a short period of heating.

Proton (^1H) and carbon (^{13}C) NMR spectra were recorded on a Bruker Avance III 400 spectrometer (Bruker Corporation, Fällanden, Switzerland) operating at 400 and 100.6 MHz, respectively. 2D experiments (^1H - ^1H COSY, NOESY, gHSQC and gHMBC) and DEPT-90/135 were run on the same instrument with the built-in Bruker pulse sequences. The solutions were prepared in CDCl_3 with chemical shifts (in ppm) referenced to tetramethylsilane in ^1H NMR spectra and/or the deuterated solvent molecules in ^{13}C NMR and 2D NMR; the abbreviations used: s – singlet, d – doublet, dd – doublet of doublets, ddd – doublet of doublet of doublets, dddd – doublet of doublet of doublet of doublets, t – triplet, tt – triplet of triplets, ddd – doublet of doublet of quartets, dqd – doublet of quartet of doublets, tdd – triplet of doublet of doublets, quint – quintet, non – nonuplet, m – multiplet (denotes complex pattern).

GC-MS analyses were performed on a Hewlett-Packard 6890N gas chromatograph equipped with a fused silica capillary column DB-5MS (5% phenylmethylsiloxane, 30 m × 0.25 mm, film thickness 0.25 μm; Agilent Technologies, Santa Clara, CA, USA) and coupled with a 5975B mass selective detector from the same company. The injector and interface were operated at 250 and 320 °C, respectively. Two temperature programs were used; program 1: oven temperature was raised from 70 to 315 °C at a heating rate of 5 °C/min and then isothermally held for 30 min; program 2: oven temperature was raised from 200 to 315 °C at a heating rate of 1 °C/min and then isothermally held for 30 min. As a carrier gas helium was used with flow 1.0 ml/min for program 1 and 1.5 ml/min for program 2. The samples, 1 μl of the sample solutions in CHCl₃ (10 mg dissolved in 1 ml), were injected in a split mode (split ratio 40:1). Mass selective detector was operated at the ionization energy of 70 eV, in the 35–850 amu range and scanning speed of 0.34 s. Relative abundance of the detected washings and fraction constituents was calculated from the peak-areas without the use of correction factors, except in the case of fatty acid methyl esters where the quantification was carried out as described below. The IR measurements (ATR – attenuated total reflectance) were carried out using a Thermo Nicolet model 6700 FTIR instrument (Waltham, Ma, USA). UV spectra (in acetonitrile) were measured using a UV-1800 UV-Vis spectrophotometer (Shimadzu, Kyoto, Japan). Elemental microanalyses for carbon and hydrogen of the synthesized compounds were carried out with a Carlo Erba 1106 microanalyzer.

4.2. Plant material

Aboveground parts (flowers and leaves of ca. 60 plants) of *Primula veris* L. (Primulaceae) were collected on the Suva Planina Mt., near Niš, in the south-east of Serbia (43.2081° N, 22.1189° E), in May 2015. The Latin binominal is given according to The Plant List: <http://www.thepiantlist.org/> (accessed on 2020). Voucher specimen was deposited in the Herbarium of the Faculty of Sciences and Mathematics, University of Niš, *Herbarium Moesiacum Niš*, under the accession numbers 13906, where a trained botanist confirmed its identity.

4.3. Flower and leaf wax washings

Fresh flowers and leaves (775 g) of *P. veris* were cleaned from dust by mild agitation. Initially, the waxes from the surface of flowers and leaves (without separation), were washed with CHCl₃ in an ultrasound bath, at room temperature. Flowers and leaves were dipped together in chloroform for no more than 5 s. The chloroform wax washings were then filtered through a Syringe Econofilter (25/0.45 lm RC, Agilent Technologies, Santa Clara, CA, USA) to remove any insoluble material, dried over anhydrous MgSO₄ and concentrated *in vacuo* to yield 926 mg of *P. veris* flowers and leaves bulk washings. Along with a portion of wax washings, a concentrated sample of the used solvent was subjected to GC-MS analysis to identify any contamination possibly arising from the use of the described procedures and/or solvents.

4.4. Chromatographic fractionation of bulk flower and leaf *P. veris* washings

Primula veris leaf and flower washings were subjected to dry-flash column chromatography using a gradient of diethyl ether (Et₂O) and *n*-hexane (from pure *n*-hexane to pure Et₂O, with an increment step of 5%, v/v; fraction volume: 100 ml). The obtained fractions were pooled according to TLC and/or GC-MS analyses. The fraction (No. 4) analyzed in detail in this work, which eluted with *n*-hexane–Et₂O (85:15, v/v) mixture (12.2 mg), R_f~0.45 (30%, v/v, diethyl ether in *n*-hexane) was initially analyzed by GC-MS and further in greater detail by NMR. The analyses revealed the presence of a series of long-chain 1-phenylalkane-1,3-diacetates, 3-oxo-1-phenyl-1-alkyl acetates, 1-phenyl-1,3-alkanediones, 1-hydroxy-1-phenyl-3-alkanones, *sec*-alkanols, and normal and

branched fatty acids. The rest of the fractions contained other classes of wax constituents, some of them ubiquitous to all plants (alkanes – fraction 1 that eluted with *n*-hexane, 77.2 mg; 2-alkanones, aldehydes and esters of FAs – fractions 2 and 3 that eluted with *n*-hexane–Et₂O (90:10, v/v), 40.5 mg, R_f~0.41 (20% diethyl ether in *n*-hexane); 1-alkanols – fraction 5 that eluted with *n*-hexane–Et₂O (80:20, v/v), 30.3 mg, R_f~0.39 (40% diethyl ether in *n*-hexane); while some constituents were characteristic of *Primula* waxes (polymethoxylated flavones, fractions 7–10, and 12 that eluted with *n*-hexane–Et₂O from 75:25, v/v to pure Et₂O, total mass 670.8 mg, R_f~0.42 (50% diethyl ether in *n*-hexane)). The constituents of several fractions (6, 11, 13–15) having a total mass of 95 mg remained unidentified.

4.5. Long-chain 1-phenylalkane-1,3-diyl diacetates, 3-oxo-1-phenyl-1-alkyl acetates, 1-phenyl-1,3-alkanediones, 1-hydroxy-1-phenyl-3-alkanones, *sec*-alkanols and fatty acids identification and/or quantification

Qualitative analysis of 1-phenylalkane-1,3-diyl diacetates, 3-oxo-1-phenyl-1-alkyl acetates, 1-phenyl-1,3-alkanediones, 1-hydroxy-1-phenyl-3-alkanones, *sec*-alkanols and fatty acids in the chloroform washings and the corresponding chromatographic fraction was based on at least three of the following five criteria: positive matches of linear retention index (RI) values (or ΔRI values for the corresponding branched-chain isomers) and of the mass spectra with those from the literature, GC co-injection experiments with authentic samples, derivatization reactions and NMR measurements. MS data for all identified long-chain compounds are given in Tables S4, S13, S15, S18, S24 and S25 in the SI document.

Quantification of the selected fatty acid methyl esters (FAMES) expressed per mg of the chromatographic fraction was carried out by the peak-area integration method. Authentic standards of saturated FAMES were injected at seven different concentrations in order to build up seven-point GC-MS calibration curves by plotting compound concentration versus peak area ($C = f(A)$). Each sample was analyzed in three consecutive runs.

All synthetic procedures concerning model compounds used for identification purposes and derivatization reactions are described, and the corresponding spectral data reported in the SI document.

Declaration of competing interest

The authors declare that they have no known competing financial interests or personal relationships that could have appeared to influence the work reported in this paper.

Acknowledgments

This work is part of the Ph.D. thesis of Milena Živković Stošić supervised by Niko Radulović. This work was funded by the Ministry of Education, Science and Technological Development of Serbia [Project No. 172061, No. contract 451-03-9/2021-14/200124].

Appendix A. Supplementary data

Supplementary data to this article can be found online at <https://doi.org/10.1016/j.phytochem.2021.112732>.

References

- Apel, L., Kammerer, D.R., Stintzing, F.C., Spring, O., 2017. Comparative metabolite profiling of triterpenoid saponins and flavonoids in flower color mutations of *Primula veris* L. *Int. J. Mol. Sci.* 18, 153. <https://doi.org/10.3390/ijms18010153>.
- Apon, J.M.B., Nicolaides, N., 1975. The determination of the position isomers of the methyl branched fatty acid methyl esters by capillary GC/MS. *J. Chromatogr. Sci.* 13, 467–473. <https://doi.org/10.1093/chromsci/13.10.467>.

- Aslam, K., Nawchoo, I.A., Bhat, M.A., Ganie, A.H., Aslam, N., 2014. Ethno-pharmacological review of genus *Primula*. *Int. J. Adv. Res.* 2, 29–34. ISSN 2320-5407.
- Bączek, K., Przybył, J.L., Mirgos, M., Kosakowska, O., Szyborska-Sandhu, I., Weglarz, Z., 2017. Phenolics in *Primula veris* L. and *P. elatior* (L.) Hill raw materials. *Int. J. Anal. Chem.* 2871579. <https://doi.org/10.1155/2017/2871579>, 2017.
- Berim, A., Gang, D.R., 2015. Methoxylated flavones: occurrence, importance, biosynthesis. *Phytochemistry Rev.* 15, 363–390. <https://doi.org/10.1007/s11101-015-9426-0>.
- Bhutia, T.D., Valant-Vetschera, K.M., 2012. Diversification of exudate flavonoid profiles in further *Primula* spp. *Nat. Prod. Commun.* 7, 587–589. <https://doi.org/10.1177/1934578X1200700509>.
- Bhutia, T.D., Valant-Vetschera, K.M., Brecker, L., 2013. Orphan flavonoids and dihydrochalcones from *Primula* exudates. *Nat. Prod. Commun.* 8, 1081–1084. <https://doi.org/10.1177/1934578X1300800812>.
- Bos, N., Dreier, S., Jørgensen, C.G., Nielsen, J., Guerrieri, F.J., d'Ettoire, P., 2012. Learning and perceptual similarity among cuticular hydrocarbons in ants. *J. Insect Physiol.* 58, 138–146. <https://doi.org/10.1016/j.jinsphys.2011.10.010>.
- British Herbal Medicine Association, 1974. *British Herbal Pharmacopoeia* (London, UK).
- Budzianowski, J., Wollenweber, E., 2007. Rare flavones from the glandular leaf exudate of the oxlip, *Primula elatior* L. *Nat. Prod. Commun.* 2, 267–270. <https://doi.org/10.1177/1934578X0700200308>.
- Budzianowski, J., Morozowska, M., Wesolowska, M., 2005. Lipophilic flavones of *Primula veris* L. from field cultivation and in vitro cultures. *Phytochemistry* 66, 1033–1039. <https://doi.org/10.1016/j.phytochem.2005.03.024>.
- Buist, P.H., 2007. Exotic biomodification of fatty acids. *Nat. Prod. Rep.* 24, 1110–1127. <https://doi.org/10.1039/b508584p>.
- Busta, L., Jetter, R., 2017. Structure and biosynthesis of branched wax compounds on wild type and wax biosynthesis mutants of *Arabidopsis thaliana*. *Plant Cell Physiol.* 58, 1059–1074. <https://doi.org/10.1093/pcp/pcx051>.
- Chinou, I., Knoess, W., Calapai, G., 2014. Regulation of herbal medicinal products in the EU: an up-to-date scientific review. *Phytochemistry Rev.* 13, 539–545. <https://doi.org/10.1007/s11101-014-9354-4>.
- Colombo, P.S., Flamini, G., Rodondi, G., Giuliani, C., Santagostini, L., Fico, G., 2017. Phytochemistry of European *Primula* species. *Phytochemistry* 143, 132–144. <https://doi.org/10.1016/j.phytochem.2017.07.005>.
- Council of Europe, 2019. European directive for the quality of medicines and health care (EDQM). In: *European Pharmacopoeia* (Ph. Eur.), tenth ed. (Strasbourg, France).
- Couperus, P.A., Clague, A.D.H., van Dongen, J.P.C.M., 1978. Carbon-13 chemical shifts of some model carboxylic acids and esters. *Org. Magn. Reson.* 11, 590–597. <https://doi.org/10.1002/mrc.1270111203>.
- Dekić, B.R., Ristić, M.N., Mladenović, M.Z., Dekić, V.S., Ristić, N.R., Randelović, V., Radulović, N.S., 2019. Diethyl-ether flower washings of *Dianthus cruentus* Griseb. (Caryophyllaceae): derivatization reactions leading to the identification of new wax constituents. *Chem. Biodivers.* 16, e1900153 <https://doi.org/10.1002/cbdv.201900153>.
- Deno, N.C., Jedziniak, E.J., Messer, L.A., Meyer, M.D., Stroud, S.G., Tomesko, E.S., 1977. The hydroxylation of alkanes and alkyl chains. *Tetrahedron* 33, 2503–2508. [https://doi.org/10.1016/0040-4020\(77\)80072-0](https://doi.org/10.1016/0040-4020(77)80072-0).
- Ejchart, A., 1981. Substituent effects on ¹³C NMR. 2-chemical shifts in the saturated framework of secondary aliphatic derivatives. *Org. Magn. Reson.* 15, 22–24. <https://doi.org/10.1002/mrc.1270150106>.
- Elser, D., Gilli, C., Brecker, L., Valant-Vetschera, K.M., 2016. Striking diversification of exudate profiles in selected *Primula* lineages. *Nat. Prod. Commun.* 11, 585–590. <https://doi.org/10.1177/1934578X1601100506>.
- Harvey, D.J., Vouros, P., 2019. Mass spectrometric fragmentation of trimethylsilyl and related alkylsilyl derivatives. *Mass Spectrom. Rev.* 1–107. <https://doi.org/10.1002/mas.21590>.
- Hoffmann, R.W., Weidmann, U., 1985. Stereoselective synthesis of alcohols, XIX. The sense of asymmetric induction on addition to α -chiral aldehydes. *Chem. Ber.* 118, 3966–3979. <https://doi.org/10.1002/chem.19851181010>.
- Huck, C.W., Huber, C.G., Ongania, K.-H., Bonn, G.K., 2000. Isolation and characterization of methoxylated flavones in the flowers of *Primula veris* by liquid chromatography and mass spectrometry. *J. Chromatogr., A* 870, 453–462. [https://doi.org/10.1016/S0021-9673\(99\)00950-4](https://doi.org/10.1016/S0021-9673(99)00950-4).
- Hwang, Y.S., Navvab-Gojrati, H.A., Mulla, M.S., 1978. Overcrowding factors of mosquito larvae. 10. Structure-activity relationship of 3-methylalkanoic acids and their esters against mosquito larvae. *J. Agric. Food Chem.* 26, 557–560. <https://doi.org/10.1021/jf60217a068>.
- Ilic-Tomic, T., Genčić, M.S., Živković, M.Z., Vasiljević, B., Djokić, L., Nikodinović-Runic, J., Radulović, N.S., 2015. Structural diversity and possible functional roles of free fatty acids of the novel soil isolate *Streptomyces* sp. NP10. *Appl. Microbiol. Biot.* 99, 4815–4833. <https://doi.org/10.1007/s00253-014-6364-5>.
- Jetter, R., Kunst, L.J., Samuels, A.L., 2006. Composition of plant cuticular waxes. In: Riederer, M., Müller, C. (Eds.), *Annual Plant Reviews Volume 23: Biology of the Plant Cuticle*. Blackwell Publishing Ltd, Germany, pp. 145–181. <https://doi.org/10.1002/9780470988718.ch4>.
- Kubinec, R., Blaško, J., Górová, R., Addová, G., Ostrovský, I., Amann, A., Soják, L., 2011. Equivalent chain lengths of all C4–C23 saturated monomethyl branched fatty acid methyl esters on methylsilicone OV-1 stationary phase. *J. Chromatogr., A* 1218, 1767–1774. <https://doi.org/10.1016/j.chroma.2011.01.065>.
- Kunst, L.J., Jetter, R., Samuels, A.L., 2006. Biosynthesis and transport of plant cuticular waxes. In: Riederer, M., Müller, C. (Eds.), *Annual Plant Reviews Volume 23: Biology of the Plant Cuticle*. Blackwell Publishing Ltd, Germany, pp. 182–215. <https://doi.org/10.1002/9780470988718.ch5>.
- L'Adapharm, 1988. *Pharmacopée Française*, tenth ed. (France).
- Masur, M., Grützmacher, H.-F., Münster, H., Budzikiewicz, H., 1987. Mass spectrometric fragmentation of the tautomers of 1,3-diketones. A gas chromatographic/mass spectrometric study. *J. Mass Spectrom.* 22, 493–500. <https://doi.org/10.1002/oms.1210220804>.
- Merad, J., Borkar, P., Caijo, F., Pons, J.-M., Parrain, J.-L., Chuzel, O., Bressy, C., 2017. Double catalytic kinetic resolution (DoCKR) of acyclic *anti*-1,3-diols: the additive hereau amplification. *Angew. Chem. Int. Ed.* 56, 16052–16056. <https://doi.org/10.1002/anie.201709844>.
- Moss, G.P., 1996. Basic terminology of stereochemistry (IUPAC Recommendations 1996). *Pure Appl. Chem.* 68, 2193–2222. <https://doi.org/10.1351/pac199668122193>.
- Niwa, M., Jiang, P.-F., Hirata, Y., 1987. Constituents of *Wikstroemia sikokiana*. II. Absolute configurations of 1,5-diphenylpentane-1,3-diols. *Chem. Pharm. Bull.* 35, 108–111. <https://doi.org/10.1248/cpb.35.108>.
- Pelter, A., Vughan-Williams, G.F., Rosser, R.M., 1993. Hindered organoboron groups in organic chemistry. 21. The reactions of dimethylboron stabilised carbanions with oxiranes. *Tetrahedron* 49, 3007–3034. [https://doi.org/10.1016/S0040-4020\(01\)80394-X](https://doi.org/10.1016/S0040-4020(01)80394-X).
- Peng, C.T., 2000. Prediction of retention indices V. Influence of electronic effects and column polarity on retention index. *J. Chromatogr., A* 903, 117–143. [https://doi.org/10.1016/S0021-9673\(00\)00901-8](https://doi.org/10.1016/S0021-9673(00)00901-8).
- Peng, C.T., 2010. Prediction of retention indices. VI: isothermal and temperature-programmed retention indices, methylene value, functionality constant, electronic and steric effects. *J. Chromatogr., A* 1217, 3683–3694. <https://doi.org/10.1016/j.chroma.2010.02.005>.
- Pretsch, E., Bühlmann, P., Badertscher, M., 2009. *Structure Determination of Organic Compounds: Tables of Spectral Data*, fourth ed. Springer-Verlag, Berlin Heidelberg, Germany.
- Radulović, N.S., Mladenović, M.Z., Stojanović, N.M., Randjelović, P.J., Blagojević, P.D., 2019. Structural elucidation of presilphiperfolene-7 α ,8 α -diol, a bioactive sesquiterpenoid from *Pulicaria vulgaris*: a combined approach of solvent-induced chemical shifts, GIAO calculation of chemical shifts, and full spin analysis. *J. Nat. Prod.* 82, 1874–1885. <https://doi.org/10.1021/acs.jnatprod.9b00120>.
- Richards, J., 2003. *Primula*, second ed. Timber Press Inc., Portland.
- Schulz, S., Arsene, C., Tauber, M., McNeil, J.N., 2000. Composition of lipids from sunflower pollen (*Helianthus annuus*). *Phytochemistry* 54, 325–336. [https://doi.org/10.1016/S0031-9422\(00\)00089-3](https://doi.org/10.1016/S0031-9422(00)00089-3).
- Shostak, L.G., Marchyshyn, S.M., Kozachok, S.S., Karbovska, R.V., 2016. Investigation of phenolic compounds of *Primula veris* L. *J. Educ. Health Sport.* 6, 424–432. <https://doi.org/10.5281/zenodo.56701>.
- Siljeström, S., Parentau, M.N., Jahnke, L.L., Cady, S.L., 2017. A comparative ToF-SIMS and GC-MS analysis of phototrophic communities collected from an alkaline silica-depositing hot spring. *Org. Geochem.* 109, 14–30. <https://doi.org/10.1016/j.orggeochem.2017.03.009>.
- Streibl, V.M., Stránský, K., 1972. Natural waxes XXII: wax ketones. *Eur. J. Lipid Sci. Technol.* 74, 566–569. <https://doi.org/10.1002/lipi.19720741002>.
- Ubik, K., Stránský, K., Streibl, V.M., 1974. Gas chromatography-mass spectrometry determination of high aliphatic secondary alcohols. *Collect. Czech Chem. Commun.* 40, 1718–1730. <https://doi.org/10.1135/cccc19751718>.
- Valant-Vetschera, K.M., Bhutia, T.D., Wollenweber, E., 2009. Exudate flavonoids of *Primula* spp: structural and biogenetic chemodiversity. *Nat. Prod. Commun.* 4, 365–370. <https://doi.org/10.1177/1934578X0900400310>.
- Van Den Dool, H., Kratz, P.D., 1963. A generalization of the retention index system including linear temperature programmed gas-liquid partition chromatography. *J. Chromatogr., A* 11, 463–471. [https://doi.org/10.1016/S0021-9673\(01\)80947-X](https://doi.org/10.1016/S0021-9673(01)80947-X).
- Wen, M., Jetter, R., 2009. Composition of secondary alcohols, ketones, alkanediols, and ketols in *Arabidopsis thaliana* cuticular waxes. *J. Exp. Bot.* 60, 1811–1821. <https://doi.org/10.1093/jxb/erp061>.
- Wollenweber, E., Mann, K., Iinuma, M., Tanaka, T., Mizuno, M., 1989. 5,2',5'-Trihydroxyflavone and 2', β -dihydroxychalcone from *Primula pulverulenta*. *Phytochemistry* 28, 295–296. [https://doi.org/10.1016/0031-9422\(89\)85067-8](https://doi.org/10.1016/0031-9422(89)85067-8).
- Xu, C., Yuan, C., 2005. *Candida rugosa* lipase-catalyzed kinetic resolution of β -hydroxy- β -arylpropionates and δ -hydroxy- δ -aryl- β -oxo-pentanoates. *Tetrahedron* 61, 2169–2186. <https://doi.org/10.1016/j.tet.2004.12.059>.
- Xu, F., Xu, J., Hu, Y., Lin, X., Wu, Q., 2016. One-pot bienzymatic cascade combining decarboxylative aldol reaction and kinetic resolution to synthesize chiral β -hydroxy ketone derivatives. *RSC Adv.* 6, 76829–76837. <https://doi.org/10.1039/C6RA12729K>.
- Zhang, L., Yan, H.-F., Wu, W., Yu, H., Ge, X.-J., 2013. Comparative transcriptome analysis and marker development of two closely related Primrose species (*Primula poissonii* and *Primula wilsonii*). *BMC Genom.* 14, 329. <https://doi.org/10.1186/1471-2164-14-329>.
- Živković, M., Genčić, M., Radulović, N.S., 2016. Comparative study of epicuticular alkane profiles of *Primula veris* L. and *P. acaulis* (L.) L. (Primulaceae). In: Randjelović, V., Stojanović-Radić, Z. (Eds.), 12th Symposium on the Flora of Southeastern Serbia and Neighboring Regions. Faculty of Sciences and Mathematics, University of Niš, Niš, pp. 88–89.
- Rezanka, T., 1992. Identification of very-long-chain acids from peat and coals by capillary gas chromatography-mass spectrometry. *J. Chromatogr., A* 627, 241–245. [https://doi.org/10.1016/0021-9673\(92\)87203-K](https://doi.org/10.1016/0021-9673(92)87203-K).